

Soil loss estimated by means of the RUSLE model in a subtropical climate watershed

Mayara Zanchin^{(1)*} , Maíra Martim de Moura⁽²⁾ , Maria Cândida Moitinho Nunes⁽³⁾ , Samuel Beskow⁽²⁾ , Pablo Miguel⁽³⁾ , Cláudia Liane Rodrigues de Lima⁽³⁾  and Danielle de Almeida Bressiani⁽²⁾ 

⁽¹⁾ Universidade Federal de Pelotas, Departamento de Solos, Programa de Pós-Graduação em Manejo e Conservação do Solo e da Água, Capão do Leão, Rio Grande do Sul, Brasil.

⁽²⁾ Universidade Federal de Pelotas, Departamento de Recursos Hídricos, Programa de Pós-Graduação em Recursos Hídricos, Pelotas, Rio Grande do Sul, Brasil.

⁽³⁾ Universidade Federal de Pelotas, Departamento de Solos, Programa de Pós-Graduação em Manejo e Conservação do Solo e da Água, Capão do Leão, Rio Grande do Sul, Brasil.

ABSTRACT: Erosion process occurs naturally, shaping the Earth's surface. Soil loss can cause harmful effects to the environment when intensive anthropic activities occur. Mathematical models have been used as effective and less costly alternatives for identifying sites highly prone to soil loss, especially at the watershed scale. In Brazil, the Revised Universal Soil Loss Equation (RUSLE) is one of the most commonly used soil loss prediction models. The RUSLE requires information on soil erodibility, rainfall erosivity, topography, land use and cover (C), and conservation practices (P) to estimate average annual soil losses. Images derived from remote sensing techniques are generally used to quantify the spatialization of C factor; however, the variation in land use throughout the year is not usually considered. This study aimed to estimate soil losses in an important subwatershed of Candiota river watershed (CRWsub) by using RUSLE, considering land use and rainfall erosivity in different periods of the year. The periods considered were P1 (January, February and March), P2 (April, May and June), P3 (July, August and September) and P4 (October, November and December). Based on the results, the lowest soil losses occurred in P1. Probably, the high vegetation cover in the soil increases its protection against rainfall erosivity. In P3, the heavy rainfall events are predominantly frontal, occurring in the same months as those when the preparation of the soil for later planting takes place; that is, there is no vegetation cover in this period, thus making the soil more prone to erosion. The use of different images to classify and identify land uses is the best way to understand soil losses throughout the year in the study area. It was possible to observe that agricultural areas are generally associated with greater soil losses in the subwatershed. In addition, the land uses were considered to vary quarterly, thereby making it possible to identify the periods most prone to erosion processes throughout the year. Finally, the erosion percentages in the subwatershed can be linked to the tolerance index for different land-uses, soil classes, and slope categories.

Keywords: spatio-temporal analysis, erosion tolerance index, Candiota river.

* Corresponding author:

E-mail: zanchinmayara@gmail.com

Received: July 05, 2021

Approved: September 16, 2021

How to cite: Zanchin M, Moura MM, Nunes MCM, Beskow S, Lima CLR, Bressiani DA. Soil loss estimated by means of the RUSLE model in a subtropical climate watershed. Rev Bras Cienc Solo. 2021;45:e0210050. <https://doi.org/10.36783/18069657rbc20210050>

Editors: José Miguel Reichert  and Luciano da Silva Souza 

Copyright: This is an open-access article distributed under the terms of the Creative Commons Attribution License, which permits unrestricted use, distribution, and reproduction in any medium, provided that the original author and source are credited.



INTRODUCTION

Soil losses result in harmful impacts onsite and offsite when anthropic activities intensify them. The loss of nutrients from the surface layers of the soil and consequent reduction in crop productivity can cause silting and eutrophication (Napoli et al., 2016; Kavian et al., 2017). According to FAO (2015), 33 % of the Earth's soils are already degraded, and the main indicators of this degradation are erosion and compaction of agricultural soils. Erosive processes cause the loss of nutrients that can lead to a loss of up to 50 % in the productivity of crops. In addition, over 90 % of the Earth's soils will be degraded until 2050 (IPBES, 2018).

Environmental laws have encouraged environmental monitoring in watersheds; however, there is still a lack of field data, which is time-consuming and costly to obtain (Batista et al., 2017). Mathematical modeling is a fast and effective tool to analyze erosion processes and establish mitigation plans. The Revised Universal Soil Loss Equation (RUSLE) (Renard et al., 1997) is a widely used worldwide equation intended for estimating soil loss (Abdo and Salloum, 2017; Swarnkar et al., 2018; Koirala et al., 2019). In Brazil, RUSLE has been widely used in different regions (Batista et al., 2017; Colman et al., 2018; Steinmetz et al., 2018).

The RUSLE estimates average annual soil loss taking into account the following factors: rainfall erosivity (R), soil erodibility (K), topography (LS), land use and cover (C), and conservation practices (P). It is possible to spatialize soil losses and broaden the understanding of erosion processes when RUSLE is applied with a Geographic Information System (GIS) (Renard et al., 1997). In this way, it becomes easier to analyze the complex relationships among the various factors controlling soil erosion (Thomas et al., 2018).

In watersheds with agricultural areas and changes in land use throughout the year, it is essential to analyze the C factor in different periods. Thus, it is important to use more than one image for the characterization of land uses from classification techniques. Several researchers have analyzed the temporal distribution of soil losses to identify the periods of the year that are the most prone to erosive processes (Bellocchi and Diodato, 2020; Rutebuka et al., 2020; Zhu et al., 2021). Understanding the temporal variations in land use helps in making decisions regarding the monitoring and management of watersheds.

An example of an area with intense agricultural activity and changes in land use throughout the year is the Candiota region, which has the largest Brazilian coal reserve and is responsible for 38 % of Brazil's coal production (Chaves et al., 2018). Furthermore, there is an important subwatershed in the region (CRWsub) that has potential for future extraction and mining activities. Because of the possible vulnerability of this watershed to undergo erosive processes, environmental monitoring and planning become essential.

This study aimed to estimate the RUSLE factors, the average quarterly soil losses, and the erosion tolerance index in the CRWsub, located in southern Brazil. Our main hypothesis is that soil losses vary throughout the year due to the changes in land use and the rainfall erosivity in different periods of the year.

MATERIALS AND METHODS

Delineation and characteristics of the study subwatershed

The study area comprises an important subwatershed of the Candiota river watershed (CRWsub), located in the city of Candiota, state of Rio Grande do Sul, Brazil (Figure 1). The CRWsub has a drainage area of 314.61 km² and a perimeter of 154.20 km. This subwatershed refers to the drainage area upstream from the ANA's water level station (code 88181000).

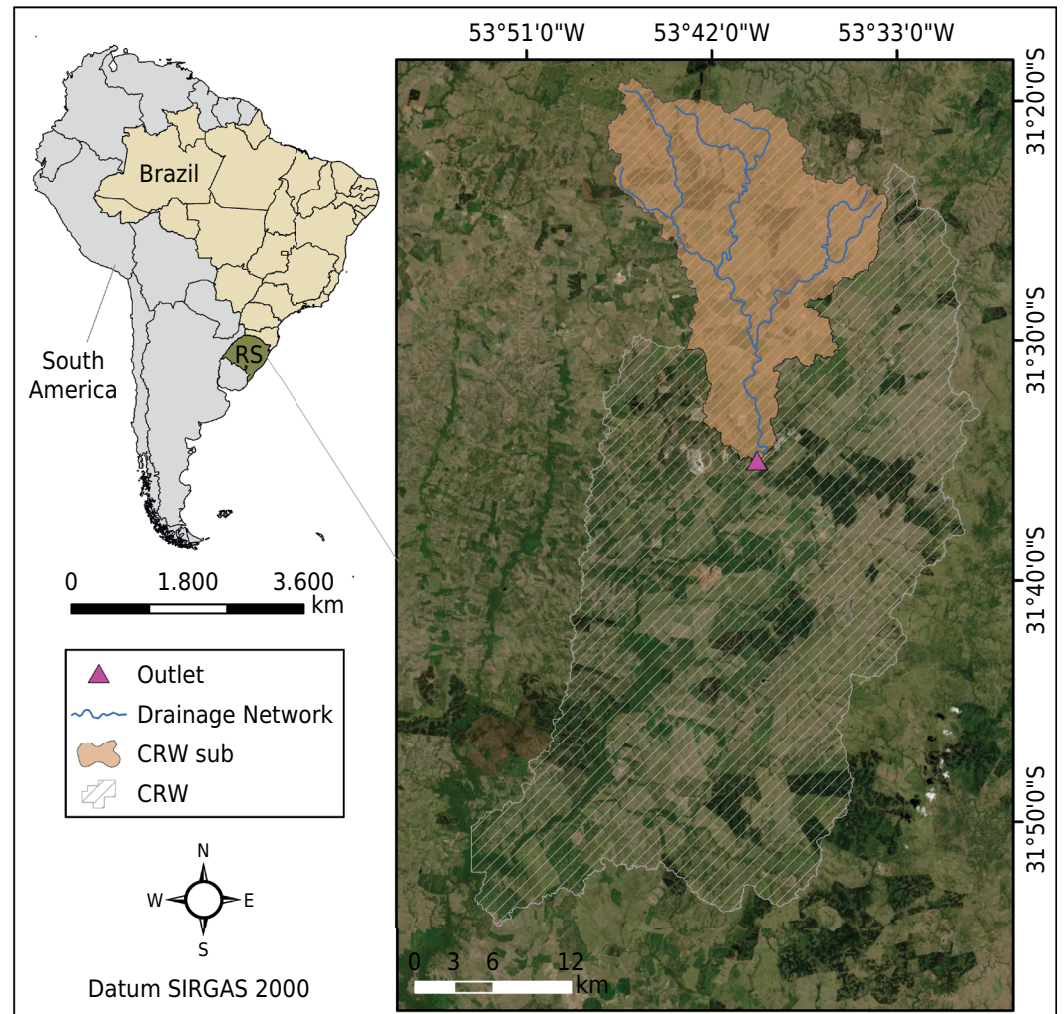


Figure 1. Location of the Candiota river watershed (CRWsub).

The region's climate is Cfa - a subtropical humid type, characterized by hot summers with temperatures above 24 °C and annual average precipitation of 1,465 mm (Alvares et al., 2014). The CRWsub is located in the *Pampa* biome, which is characterized by pastures and high biodiversity of fauna and flora (Lupatini et al., 2013).

The study area is characterized by the presence of poorly developed soils compounds of some rock outcrops associated with Eutric Leptsol and Leptic Regosol (Cunha et al., 2006; IUSS Working Group WRB, 2015). This corresponds to the association between *Afloramento Rochoso* + *Neossolo Litólico Eutrófico típico* + *Neossolo Regolítico Distrófico léptico*, according to the Brazilian Soil Classification System - SiBCS (Santos et al., 2018). Soils with an argic horizon were also found, such as Abruptic Acrisol, Haplic Lixisol and Abruptic Alisol, which correspond to *Argissolo Vermelho-Amarelo Distrófico típico*, *Argissolo Vermelho Eutrófico típico*, and *Argissolo Amarelo Distrófico típico*, respectively (Figure 2a). Other soils found in lower percentages in the area were soils with mollic horizon such as Someric Phaeozem (*Chernossolo Háptico Órtico típico*); poorly drained soils, such as Reductic Gleysol (*Gleissolo Melânico Ta Eutrófico planossólico vertissólico*) and Eutric Leptsol (*Neossolo Litólico Eutrófico típico*). The percentages of each soil class in the CRWsub are: Rock Outcrops (12.57 % - associated with Eutric Leptsol + Leptic Regosol); Abruptic Acrisol (44.39 %); Haplic Lixisol (18.77 %); Abruptic Alisol (8.09 %); Someric Phaeozem (6.41 %); Reductic Gleysol (5.23 %) and Eutric Leptsol (4.54 %).

The delineation and characterization of the CRWsub were performed automatically in the software ArcGIS 10.1[®] (ESRI, 2014), following the procedures proposed by Ray (2018).

It was used a digital elevation model (DEM) derived from the Shuttle Radar Topographic Mission (SRTM) (Farr et al., 2007) with a spatial resolution of 30 m (Figure 2b). The altitudes in the CRWsub range from 166 to 406 m, and the average slope is equal to 7.74 %. The CRWsub presents 57.44 and 39.56 % of the area, respectively, in low (0 - 8 %) and medium (8 - 20 %) slopes, and 3 % is classified as a high (20 - 45 %) slope, according to the classification suggested by Embrapa (1979) (Figure 2c).

Land use classification

Preliminary field campaigns were carried out to identify the existing land uses and management of soils. Subsequently, a supervised image classification was conducted considering 30 m resolution images for the orbit-point 222082 from the Enhanced Thematic

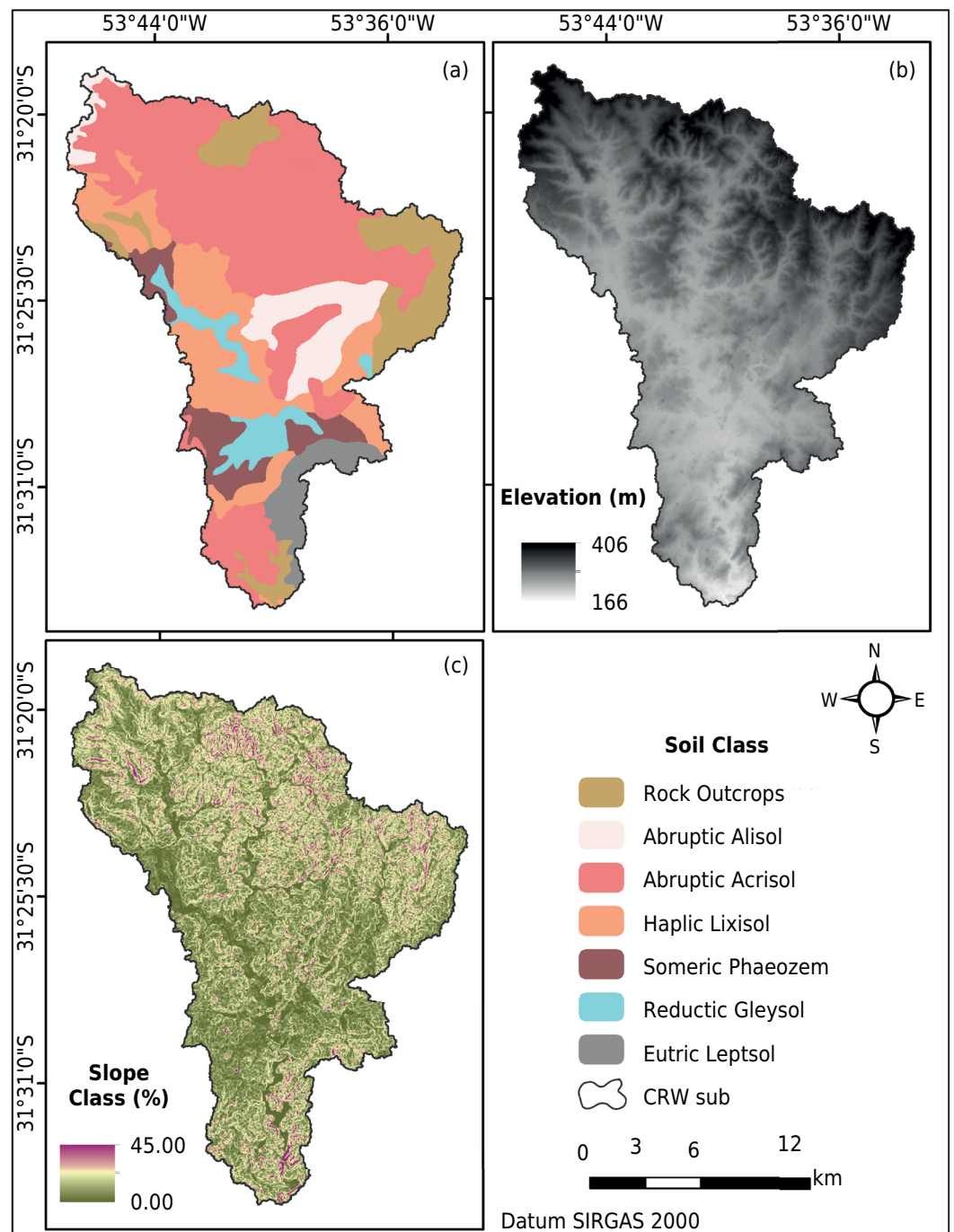


Figure 2. Indication of (a) digital elevation model; (b) slope and (c) soil classes in the Candiota river watershed (CRWsub). The soil classes were compared to the WRB classification (2015).

Mapper Plus (ETM+) and Operational Land Imager (OLI) sensors of the Landsat 7 and Landsat 8 satellites, respectively. The final quality of the classification was assessed by a confusion matrix and the Kappa Index (I_k), as performed by Kaviani et al. (2017) and Abdo and Salloum (2017). The supervised classification was performed using ArcGIS software (ESRI, 2014). False-color composites were used in the study because they are more recommended to analyze land use and cover (Kou et al., 2015). Thus, the multispectral bands used for Landsat 7 were 5-4-3, and for Landsat 8, the equivalent composition 6-5-4 was used. A classification of 16 land use images was carried out, one for each quarter of the year from 2013 to 2016, with the following periods of analysis: P1 - January to March; P2 - April to June; P3 - July to September; and P4 - October to December. Information regarding the images used can be found in table 1.

Revised Universal Soil Loss Equation (RUSLE)

The methodology used to estimate average annual soil loss was proposed by Renard et al. (1997) (Equation 1), referred to as Revised Universal Soil Loss Equation (RUSLE).

$$A = R K L S C P \quad \text{Eq. 1}$$

in which: A is the average annual soil loss per unit area ($\text{Mg ha}^{-1} \text{yr}^{-1}$), R corresponds to the rainfall erosivity factor ($\text{MJ mm ha}^{-1} \text{h}^{-1} \text{yr}^{-1}$), K refers to the soil erodibility factor ($\text{Mg h MJ}^{-1} \text{mm}^{-1}$), LS is the topographic factor (dimensionless) and CP means the cover factor (use and cover) and soil conservation practices (dimensionless).

RUSLE is generally applied in an annual timestep. However, due to the different rainfall patterns and land use throughout the year experienced in the study area, the period of analysis proposed in this study was quarterly ($A = \text{Mg ha}^{-1} \text{quarter}^{-1}$). Therefore, some variables were modified in relation to units as follows: erosivity factor ($R = \text{MJ mm ha}^{-1} \text{h}^{-1} \text{quarter}^{-1}$) and cover factor (one image was analyzed for each quarter of the year, totaling 16 land use images).

Erosivity factor (R)

Erosivity is the potential of rainfall to erode bare soil (Renard et al., 1997). Soil losses are related to the erosivity index (EI30), which is the product of the total kinetic energy (E) by the average maximum intensity of 30-minute rainfall (I30) (Koirala et al., 2019). The erosivity index is one of the best indicators for quantifying the rainfall erosive potential.

Determination of the EI30 using rainfall intensity data is laborious because extensive and consistent data series are necessary to determine the kinetic energy and the maximum intensity of the rainfall events. Since there is a lack of data from self-recording rain gauges, mainly at the national level, daily rainfall data from non-recording rain gauges have been used to estimate the EI30 (Santos and Montenegro; 2012; Back et al., 2017). Thus, it is possible to correlate the EI30 with the Fournier's index, established as the

Table 1. Date of acquisition of Landsat 7 and Landsat 8 images used for C factor analyses, in the following periods: P1 - January to March; P2 - April to June; P3 - July to September; and P4 - October to December

Periods	Year			
	2013	2014	2015	2016
P1	03/06*	01/28	02/08	01/18
P2	05/17	06/21	05/07*	06/18*
P3	08/05	09/25	09/12	08/13
P4	10/08	10/27	11/15	12/11*

* Date from Landsat 7.

rainfall coefficient (R_c), which represents the relationship between the square of monthly average rainfall and annual average rainfall (Equation 2). We opted for the equation developed by Peñalva-Bazzano et al. (2007) to estimate rainfall erosivity from daily rainfall data (Equation 3). This equation was obtained from rainfall data monitored in a city close to Candiota.

$$R_c = \frac{p^2}{P} \quad \text{Eq. 2}$$

$$EI30 = -47.35 + [82.72 R_c] \quad \text{Eq. 3}$$

in which: EI30 is the erosivity index ($\text{MJ mm ha}^{-1} \text{h}^{-1}$); R_c is Fournier's rainfall coefficient (mm); p is average monthly rainfall (mm) and P is average annual rainfall (mm).

We used the historical rainfall series from the Bagé meteorological station (code 83980) from 1961 to 2019, monitored by the Brazilian National Institute of Meteorology. Rainfall erosivity was analyzed on quarterly and annual time steps, as agricultural practices, cultivation systems, and rainfall patterns are different throughout the year in this area. The annual erosivity values ($\text{MJ mm ha}^{-1} \text{h}^{-1} \text{yr}^{-1}$) were classified according to the methodology adapted from Carvalho (2008): $R < 2452$: low; $2452 \leq R < 4905$: weak; $4905 \leq R < 7357$: moderate; $7357 \leq R < 9810$: strong; and $R \geq 9810$: very strong.

Soil erodibility

Soil erodibility (K) represents the intrinsic susceptibility to soil erosion, determined by annual soil loss and annual rainfall erosivity (Cassol et al., 2018). The soil classes that are present in the CRWsub were identified from the soil map prepared by Cunha et al. (2006). The values used for K were the same as those presented by Zanchin (2020), whose literature review prioritized studies with field experiments. The K values ($\text{Mg h MJ}^{-1} \text{mm}^{-1}$) adopted were: Rock Outcrops (0.0087); Abruptic Acrisol (0.0338); Haplic Lixisol (0.0351); Abruptic Alisol (0.0215); Someric Phaeozem (0.0385); Reductic Gleysol (0.0395); Eutric Leptsol (0.0463) and Leptic Regosol (0.0409).

Topographic factor

Topographic factor (LS) represents the effects of topography on soil loss. Factor L indicates the impact of the slope length, whereas, the factor S represents the effect of terrain slope on soil losses (Wischmeier and Smith, 1978). One of the widely used methodologies (Equation 4) for calculating the LS factor is that proposed by Moore and Burch (1986) (Hrabalíková and Janeček, 2017; Zanin et al., 2017), which allows the spatial representation of the LS factor in areas of complex relief such as watersheds (Minella et al., 2010). Equation 4 was established in ArcGIS 10.1 (ESRI, 2014) through the *Raster Calculator*.

$$LS = \left[\left(\frac{FA_i b}{22.13} \right)^{0.40} \left(\frac{\sin(\alpha)}{0.0896} \right)^{1.3} \right] \quad \text{Eq. 4}$$

in which: FA is the accumulated flow in cell i , b is the spatial resolution of the cell (m), and α is the slope (degrees).

Cover management and conservation practice factors

Land cover and conservation practices factor (CP) represents the anthropic intervention in the control of soil loss associated with different land covers. Cover (C) refers to the joint impacts of intense use and inadequate management on soil loss rates. Conservation practices (P) represent the effect of complementary conservation practices to control soil loss, compared to the corresponding soil loss when the crop is established in the direction of the slope (Didoné et al., 2015).

Values selected for the land cover and conservation practices factors were those proposed by Zanchin (2020), such that the choices were based on data from experiments carried out in the field. The values used were: pasture (0.500), annual crop (0.212), bare soil (1.000), water body (0.000), reforestation (0.122) and native vegetation (0.015). Due to the difficulty in obtaining the conservation practices factor through satellite images, the value of $P = 1$ was used (Batista et al., 2017).

Estimation of soil loss

Average soil loss in the CRWsub was analyzed on quarterly and annual time steps, taking as reference the period from 2013 to 2016. Knowledge of soil loss at different time scales is essential for planning and environmental management in watersheds. Thus, it is possible to identify the most appropriate soil and water management and conservation systems, aiming to minimize negative effects and soil losses.

Erosion tolerance index

Identification of regions under critical erosion conditions was conducted using the erosion tolerance index (ETI) (Sudhishri et al., 2014; Ghafari et al., 2017), which expresses the ratio between soil loss tolerance and the annual rate of soil loss in the watershed. The use of the ETI makes it possible to quantify how much the soil losses are beyond the tolerance, without the need to adopt arbitrary classifications, as they vary with the local geomorphology.

Soil loss tolerance values used in the present study were presented by Zanchin (2020) in $\text{Mg ha}^{-1} \text{yr}^{-1}$. The author prioritized data from experiments carried out in the field, namely: Rock Outcrops (2.63); Abruptic Acrisol (9.39); Haplic Lixisol (11.01); Abruptic Alisol (10.00); Someric Phaeozem (13.13); Reductic Gleysol (8.70); and Eutric Leptsol + Leptic Regosol (5.26).

Tolerance index was used to classify the potential for soil loss, according to the classification suggested by Ghafari et al. (2017): $\text{ETI} > 1$: very low; $0.8 < \text{ETI} \leq 1$: low; $0.5 < \text{ETI} \leq 0.8$: medium, and $\text{ETI} \leq 0.5$: high. According to the authors, ETI values ≤ 0.5 indicate that the soil loss exceeds more than twice the limit value of tolerance for soil losses. It is worth mentioning that no studies were found in Brazil involving the ETI until the completion of this study.

RESULTS

Image classification

Table 2 shows the average values obtained between 2013 and 2016 for each type of land use classified in the CRWsub.

Soil loss (A) and erosion tolerance index (ETI)

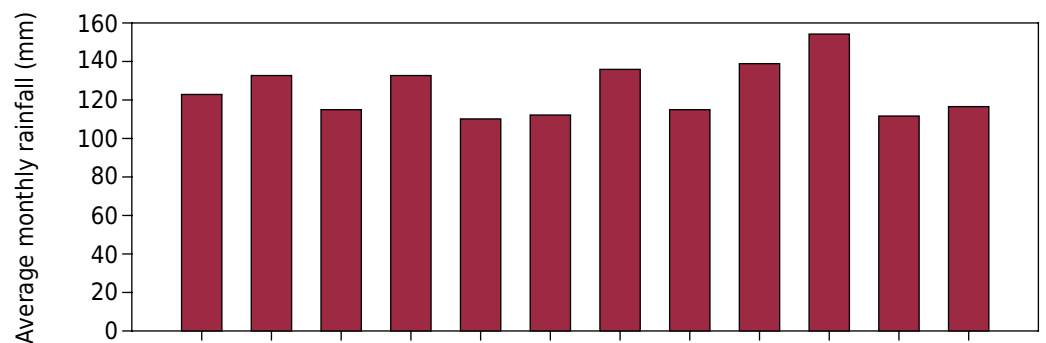
Average annual rainfall erosivity obtained for the CRWsub was equal to $9960.52 \text{ MJ mm ha}^{-1} \text{ h}^{-1} \text{ yr}^{-1}$, classified as very strong (Carvalho, 2008). The average quarterly rainfall erosivity values were: P1: 2418.38; P2: 2212.34; P3: 2699.30, and P4: $2630.50 \text{ mm ha}^{-1} \text{ h}^{-1} \text{ quarter}^{-1}$ (Figure 3). The values obtained for the LS factor varied between 0 and 32.62, with an average equal to 3.

Average quarterly soil loss values were: P1: 42.3; P2: 66.7; P3: 70.4, and P4: $54.8 \text{ Mg ha}^{-1} \text{ quarter}^{-1}$ (Figure 4). The average ETI values were computed for each period and for each soil class present in the CRWsub. The average ETI ranged between 0.67 and 7.24 (Table 3). Table 4 presents the areas of the CRWsub occupied for different land uses, soil classes and degrees of slope in relation to the tolerance index.

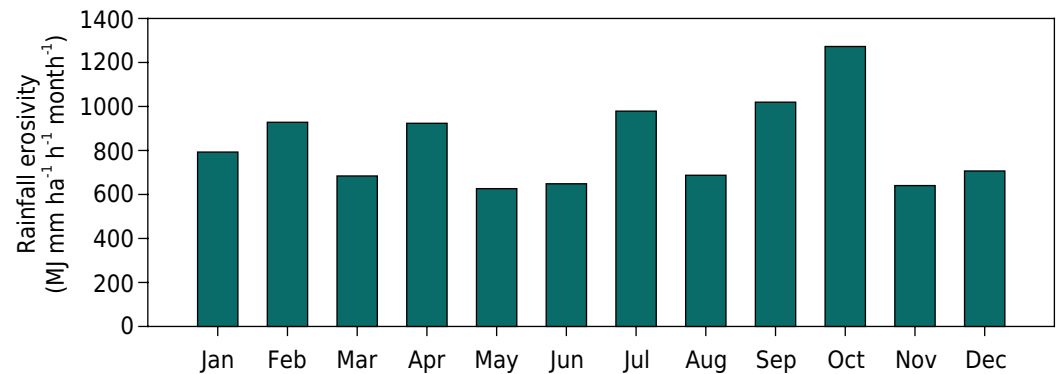
Table 2. Average values of the land use class in the CRWsub

Land Use Class	Area			
	P1	P2	P3	P4
	%			
Native Forest	8.01	7.56	7.41	6.45
Grassland	66.91	67.19	60.22	58.74
Reforestation	8.46	7.87	7.58	8.28
Annual Cropping	9.05	5.51	7.95	14.77
Bare Soil	5.81	10.11	15.08	10.00
Water Body	1.76	1.76	1.76	1.76

(a)



(b)


Figure 3. Analysis of (a) average monthly rainfall and (b) rainfall erosivity in the Candiotia region.

DISCUSSION

Image classification

Through the visual classification of images, the predominant land use in the CRWsub over the four years of analysis and at different periods of the year was pasture, followed by agriculture (P1 and P4) and bare soil (P2 and P3) (Table 2). These land uses corroborate those found by Farias et al. (2015) for this watershed.

Variations in the estimated values of soil loss are largely related to the percentages of bare soil (P3) and the type of agricultural cultivation (P4). Due to the impact of these activities, the tendency is to increase soil losses when such land uses are combined with high rainfall intensity and soils with low tolerance to erosion processes.

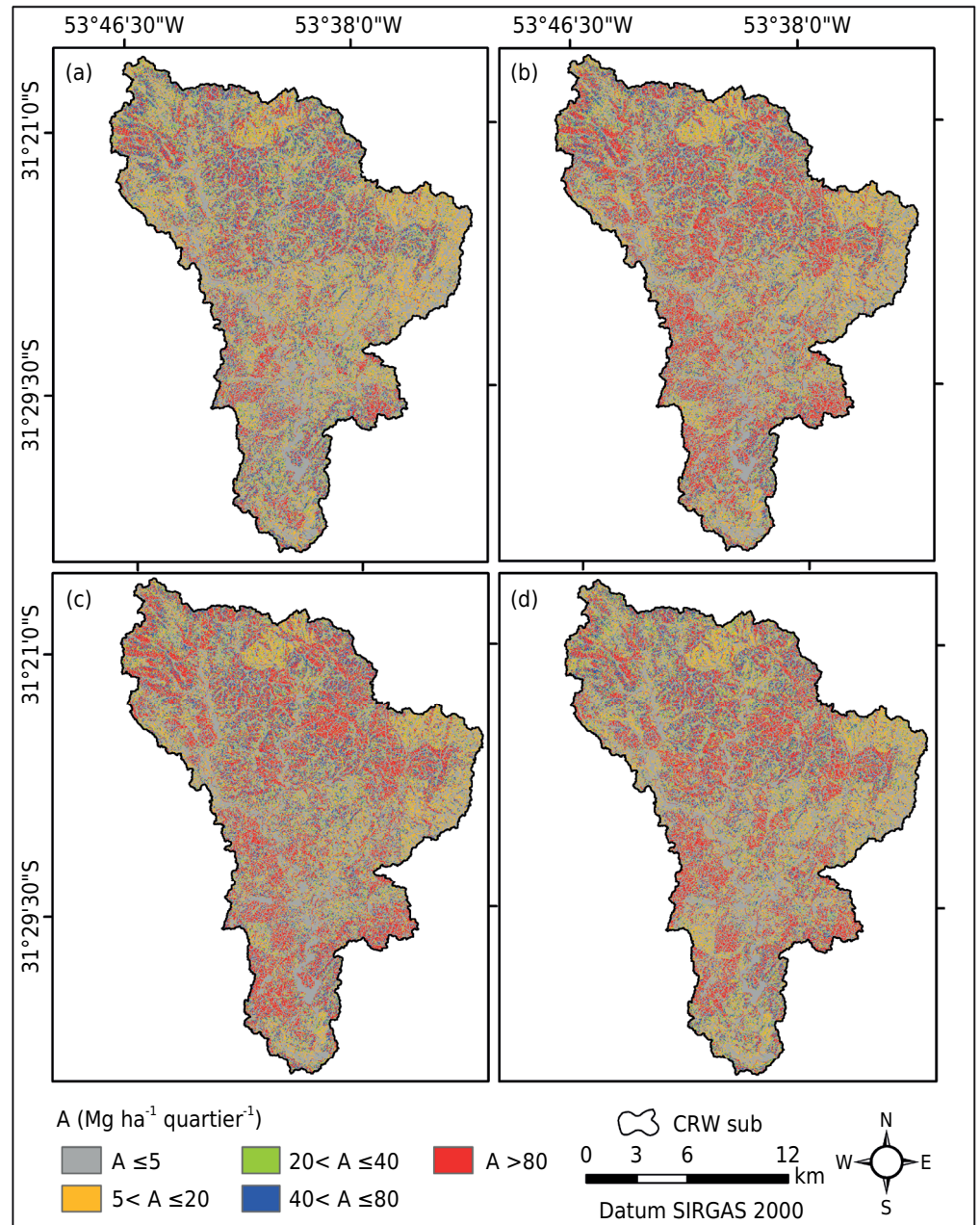


Figure 4. Soil loss ($A - \text{Mg ha}^{-1} \text{quartier}^{-1}$) in (a) P1; (b) P2; (c) P3 and (d) P4 in the Candiota river watershed (CRWsub).

Table 3. Soil loss (A) and erosion tolerance index (ETI) for the soil classes present in the Candiota river watershed (CRWsub)

Soil Class	A				ETI			
	P1	P2	P3	P4	P1	P2	P3	P4
	————— $\text{Mg ha}^{-1} \text{quartier}^{-1}$ —————							
Rock Outcrops	1.15	1.05	1.40	1.49	2.30	2.52	1.88	1.77
Abruptic Acrisol	3.64	3.50	4.55	4.45	2.59	2.68	2.07	2.11
Haplic Lixisol	2.76	2.67	3.62	3.56	3.99	4.13	3.08	3.10
Abruptic Alisol	1.74	1.64	2.25	2.28	5.76	6.11	4.46	4.40
Someric Phaeozem	2.11	1.99	2.59	2.65	6.25	6.62	5.19	5.06
Reductic Gleysol	1.21	1.22	1.49	1.59	7.24	7.17	6.00	5.51
Eutric Leptosol	6.04	5.76	7.69	7.95	0.87	0.92	0.69	0.67

Table 4. Percentages of the area in the Candiota river watershed (CRWsub) according to the ETI classification relation to land slope, soil class and use

Interest Factors		Very Low	Low	Medium	High	Total
		Area				
		%				
Slope Class	Low (0 - 8 %)	42.46	4.09	5.28	8.40	60.24
	Medium (8 - 20 %)	13.10	1.20	2.80	19.05	36.15
	High (20 - 45 %)	0.84	0.26	0.42	2.10	3.61
Soil Class	Rock Outcrops	5.56	2.06	1.25	3.70	12.57
	Abruptic Acrisol	20.00	5.60	6.74	12.05	44.39
	Haplic Lixisol	9.23	1.93	2.32	5.29	18.77
	Abruptic Alisol	4.44	1.43	0.47	1.75	8.09
	Someric Phaeozem	3.96	1.04	0.38	1.03	6.41
	Reductic Gleysol	2.14	1.19	0.85	1.05	5.23
	Eutric Leptsol	1.56	0.33	0.49	2.16	4.54
Land Use Class	Water Body	1.76	0.00	0.00	0.00	1.76
	Native Forest	5.78	0.73	0.69	0.16	7.36
	Grassland	35.00	16.09	3.02	9.15	63.26
	Reforestation	3.62	0.96	1.41	2.06	8.05
	Annual Cropping	3.67	0.38	0.95	4.32	9.32
	Bare Soil	2.10	0.29	0.39	7.47	10.25

Soil loss

The average annual erosivity value ($9960.52 \text{ MJ mm ha}^{-1} \text{ h}^{-1} \text{ yr}^{-1}$) is in agreement with the values obtained by other authors for locations close to the area of this study (Peñalva-Bazzano et al., 2007; Martins et al., 2009). When analyzing a quarterly watershed, the R values demonstrated the heterogeneity of rainfall over the months in the CRWsub and, consequently, the greater variation in the values soil loss. This finding goes along with the results found by Cordeiro et al. (2019), who observed high interannual variability in the region's rainfall regime when evaluating historical rainfall data (1961 to 2016) from Bagé (RS).

Despite the high rainfall depths in P1, this period does not hold the highest rainfall erosivity values in the CRWsub (Figure 3). The highest values of erosivity occurred in P3 and P4. Considering that the Fournier index was applied in this study, the result may be related to the predominance of frontal rainfall systems, increasing the rainfall depths in this period of the year in Rio Grande do Sul State (Wollmann, 2014).

The LS factor allows to observe the variation of the flatter locations in relation to the steeper areas. Despite varying from 0 to 32.62, the LS values obtained for the CRWsub indicate low ($LS \leq 1$) or very low ($1 < LS \leq 2$) susceptibility to erosion in 77 % of the area, according to Fornelos and Neves (2007). Following the same classification, only 4.5 % of the watershed has LS with strong susceptibility to erosion ($LS > 10$).

Soils with argic horizon comprise about 72 % of the total area in the CRWsub, and are mostly found in medium- to high-slope regions (8–45 %). Reductic Gleysols, Eutric Leptsols and Someric Phaeozem soils are found in small areas of the watershed and are located in regions with a predominance of low slopes (0–8 %).

Eutric Leptsols had the greatest soil losses, followed by soils with argic horizon (Abruptic Acrisol and Haplic Lixisol) (Table 3). It is known that Leptsols tend to be shallow and

abundant in rock fragments (Corado Neto et al., 2015). Thus, even in flat areas in the CRWsub, these soils offer few resistances to the erosion process, probably due to the low aggregation. Sartori et al. (2005) suggested that soils with argic horizon have low resistance and low tolerance to soil loss. In most of these soils, there is a texture gradient, promoting high direct surface runoff and erodibility. The lowest soil losses were identified in the Rock Outcrops and Reductic Gleysols. Even in association with Eutric Leptsol and Leptic Regosol, it is known that rock outcrops do not experience soil losses (Steinmetz et al., 2018), contributing to the low estimated values.

The lowest soil losses occurred in P1 and the highest in P3. The P1 is marked by the beginning of flowering and filling of soybeans (predominant crop), which leads to the expansion of land cover and protection against the impact of raindrops and direct surface runoff. The P3 refers to the period of soil preparation for later planting, when the soil is more susceptible to erosion, mainly due to the removal of the vegetation cover and soil revolving. Nachtigall et al. (2020) observed that greater soil losses in RS occur in the spring period, corroborating the results found in the present study. The results are explained due to the agroclimatic seasonal variation in the region.

In southern Brazil, monthly variations in rainfall and land use are observed. Therefore, the estimation of soil loss over shorter periods such as quarterly is a useful strategy. Some authors have indicated that it is possible to determine the periods of the year and the area most susceptible to soil loss with greater precision, when using the seasonality effect on RUSLE factors (Buriol et al., 2013; Moura-Bueno et al., 2018; Nachtigall et al., 2020).

Erosion tolerance index (ETI)

Among soils, Eutric Leptsols and Rock Outcrops had low ETI values, representing high potential for soil loss (Table 4). The soil type with greater loss tolerance was Someric Phaeozem and Reductic Gleysol. Even though some Someric Phaeozem may have a texture gradient, these soils do not have a texture gradient in the CRWsub, thereby favoring saturation with water (Sartori et al., 2005). In addition, both are naturally located on flat sites.

The ETI values between soil classes within the same period showed very small differences. Despite this, the ETI values between the analyzed periods indicated considerable differences (Table 3). High ETI values were observed for all soil classes in P2. There is a tendency for reduction in soil loss in relation to tolerance in this period. This is possibly due to lower rainfall erosivity values in the months of P2 and the high soil coverage with pasture in this period of year. On the other hand, lower values of ETI were observed in P3 and P4, suggesting that soil losses tend to be greater than the tolerated values. This is due to the high rainfall erosivity between October and December; combined with the scarcity of vegetation cover on the soil, since the crops are in the planting (P3) and emergence (P4) periods.

When the ETI is analyzed by slope classes according to area percentage (Table 4), it was found that most of the CRWsub had very low ETI (56.40 %), however, approximately 30 % of the CRWsub is classified as high ETI (ETI <0.5) in areas of greater slopes, combined with bare soil or agricultural activity, and in soils with high susceptibility to losses. As analyzed, agricultural areas occupy the largest extent of the basin. So, it is recommended to adopt practices that minimize soil losses in these areas, such as the use of terrain contours on slopes and the implementation of a no-till.

These findings revealed that, for identifying the high hazard areas for soil erosion, more studies are needed involving the erosion tolerance index (ETI) in Brazil. The results of this study are useful for officials and policy makers of soil conservation and environmental protection agencies in the region.

CONCLUSION

Use of different images for the classification and identification of land uses is the best way to understand soil losses throughout the year in the study area. Agricultural areas are generally associated with greater soil losses in the subwatershed. Since land uses were considered to vary quarterly, periods most prone to erosion processes throughout the year were identified. Erosion percentages in the subwatershed can be linked to the tolerance index for different land uses, soil classes, and slope categories.

ACKNOWLEDGMENTS

The authors wish to thank the Coordenação de Aperfeiçoamento de Pessoal de Nível Superior (CAPES) and Fundação de Amparo à Pesquisa do Estado do Rio Grande do Sul (FAPERGS) for the scholarships to the first and second authors. The publication of this paper was partially supported by PRPPGI/UFPel and CAPES. The authors would also wish to thank Luis Eduardo, Environment Manager at CGTEE, for providing the data required.

AUTHOR CONTRIBUTIONS

Conceptualization:  Maria Cândida Moitinho Nunes (equal) and  Samuel Beskow (equal).

Data curation:  Maíra Martim de Moura (equal) and  Mayara Zanchin (equal).

Formal analysis:  Maíra Martim de Moura (equal) and  Mayara Zanchin (equal).

Investigation:  Mayara Zanchin (lead).

Methodology:  Maíra Martim de Moura (equal),  Maria Cândida Moitinho Nunes (equal),  Mayara Zanchin (equal) and  Samuel Beskow (equal).

Project administration:  Maria Cândida Moitinho Nunes (equal),  Samuel Beskow (equal).

Software:  Maíra Martim de Moura (equal) and  Mayara Zanchin (equal).

Supervision:  Maria Cândida Moitinho Nunes (equal),  Maíra Martim de Moura (equal) and  Samuel Beskow (equal).

Writing - original draft:  Cláudia Liane Rodrigues de Lima (equal),  Danielle de Almeida Bressiani (equal),  Maria Cândida Moitinho Nunes (equal),  Maíra Martim de Moura (equal),  Mayara Zanchin (equal),  Pablo Miguel (equal) and  Samuel Beskow (equal).

REFERENCES

- Abdo H, Salloum J. Mapping the soil loss in Marqya basin: Syria using the RUSLE model in GIS and RS techniques. *Environ Earth Sci.* 2017;76:104-14. <https://doi.org/10.1007/s12665-017-6424-0>
- Alvares CA, Stape JL, Sentelhas PC, Gonçalves JLM, Sparovek G. Koppen's climate classification map for Brazil. *Meteorol Z.* 2014;22:711-28. <https://doi.org/10.1127/0941-2948/2013/0507>
- Back AJ, Pola AC, Ladwig NI, Schwalm H. Erosive rainfall in Rio do Peixe Valley in Santa Catarina, Brazil: Part I - Determination of the erosivity index. *Rev Bras Eng Agri Amb.* 2017;21:774-9. <https://doi.org/10.1590/1807-1929/agriambi.v21n11p774-779>
- Batista PVG, Naves Silva ML, Christofaro Silva BP, Curi N, Bueno IT, Acérbi Júnior FW, Davies J, Quinton J. Modelling spatially distributed soil losses and sediment yield in the upper Grande River Basin - Brazil. *Catena.* 2017;157:139-50. <https://doi.org/10.1016/j.catena.2017.05.025>

- Bellocchi G, Diodato N. Rainfall erosivity in soil erosion processes. *Water*. 2020;12:722-30. <https://doi.org/10.3390/w12030722>
- Buriol GA, Stefanel V, Swarowsky A, Cademartori RTO. Homogeneidade espacial da precipitação pluvial na bacia hidrográfica do Rio Vacacaí, RS. *Cienc Rural*. 2013;43:2160-7. <https://doi.org/10.1590/S0103-84782013005000131>
- Carvalho NO. Hidrossedimentologia prática. Rio de Janeiro: Interciência; 2008.
- Cassol EA, Silva TS, Eltz FLF, Levien R. Soil erodibility under natural rainfall conditions as the K factor of the universal soil loss equation and application of the nomograph for a subtropical Ultisol. *Rev Bras Cienc Solo*. 2018;42:e0170262. <https://doi.org/10.1590/18069657rbcs20170262>
- Chaves HAF, Rodrigues R, Ade MVB. Geochemical characterization of coal deposits of Candiota coalfield Rio Bonito Formation (E-Permian) of Paraná Basin, South Brazil. *J Soils Sediments*. 2018;3:19-35. <https://doi.org/10.12957/jse.2018.33240>
- Colman CB, Garcia KMP, Pereira RB, Shinma EA, Lima FE, Gomes AO, Oliveira PTS. Different approaches to estimate the sediment yield in a tropical watershed. *Rev Bras Recur Hid*. 2018;23:e47. <https://doi.org/10.1590/2318-0331.231820170178>
- Corado Neto FC, Sampaio FMT, Veloso MEC, Matias SSR, Andrade FR, Lobato MGR. Variabilidade espacial da resistência à penetração em Neossolo Litólico degradado. *Rev Bras Cienc Solo*. 2015;39:1353-61. <https://doi.org/10.1590/01000683rbcs20140692>
- Cordeiro APA, Marques Alves RC, Rocha MB. Caracterização agroclimática de Bagé, RS. *Agrometeoros*. 2019;27:293-309. <https://doi.org/10.31062/agrom.v27i2.26470>
- Cunha NG, Silveira RJC, Severo CRC. Solos e terras do planalto Sul-Rio-Grandense e planícies costeiras. Pelotas: Embrapa Clima Temperado; 2006.
- Didoné EJ, Minella JPG, Merten GH. Quantifying soil erosion and sediment yield in a catchment in southern Brazil and implications for land conservation. *J Soils Sediments*. 2015;15:2334-46. <https://doi.org/10.1007/s11368-015-1160-0>
- Empresa Brasileira de Pesquisa Agropecuária (EMBRAPA). *Súmula da X Reunião Técnica de Levantamento de Solos*. 1a ed. Rio de Janeiro: Serviço Nacional de Levantamento e Conservação de Solos; 1979.
- Environmental Systems Research Institute - ESRI. *ArcGIS for Desktop, Version 10.1 [CD ROM]*. Redlands: ESRI; 2014.
- Food and Agriculture Organization (FAO). *Status of the world's soil resources (SWSR) - main report [internet]*. Food and agriculture Organization of the United Nations, Italy; 2015 [cited 2020 Dec 02]. Available from: <http://www.fao.org/3/a-i5199e.pdf>
- Farias RN, Pedrozo CS, Machado NAF, Rodriguez MTR. Análise morfológica e de usos do solo da bacia hidrográfica do Arroio Candiota, RS, Brasil. *Pesqui Geocienc*. 2015;42:159-72. <https://doi.org/10.22456/1807-9806.78117>
- Farr TG, Rosen PA, Caro E, Crippen R, Duren R, Hensley S, Kobrick M, Paller M, Rodriguez E, Roth L, Seal D, Shaffer S, Shimada J, Umland J, Werner M, Oskin M, Burbank D, Alsdorf D. The shuttle radar topography mission. *Rev Geophys*. 2007;45:RG2004. <https://doi.org/10.1029/2005RG000183>
- Fornelos LF, Neves SMA. Uso de modelos digitais de elevação (MDE) gerados a partir de imagens de radar interferométrico (SRTM) na estimativa de perdas de solo. *Rev Bras Cartogr*. 2007;59:25-33
- Ghafari H, Gorji M, Arabkhedri M, Ali GR, Heidari A, Akhavan S. Identification and prioritization of critical erosion areas based on onsite and offsite effects. *Catena*. 2017;156:1-9. <https://doi.org/10.1016/j.catena.2017.03.014>
- Hrabalíková M, Janeček M. Comparison of different approaches to LS factor calculations based on a measured soil loss under simulated rainfall. *Soil Water Res*. 2017;12:69-77. <https://doi.org/10.17221/222/2015-SWR>
- Intergovernmental Science-Policy Platform on Biodiversity and Ecosystem Services (IPBES). *The assessment report on: Land degradation and restoration. Summary for policymakers [internet]*. IPBES, Germany; 2018 [cited 2020 May 15]. Available from: https://ipbes.net/sites/default/files/2018_ldr_full_report_book_v4_pages.pdf

- International Union of Soil Science (IUSS) Working Group WRB. International soil classification system for naming soils and creating legends for soil maps [internet]. World Reference Base for Soil Resources, universal system recognized by International Union of Soil Science (IUSS) e FAO; 2015 [cited 2020 May 13]. Available from: <http://www.fao.org/3/a-i3794e.pdf>.
- Kavian A, Sabet SH, Solaimani K, Jafari B. Simulating the effects of land use changes on soil erosion using the RUSLE model. *Geocarto Int.* 2017;32:97-111. <https://doi.org/10.1080/10106049.2015.1130083>
- Koirala P, Thakuri S, Joshi S, Chauhan R. Estimation of soil erosion in Nepal using a RUSLE modeling and geospatial tool. *Geosciences.* 2019;9:147-53. <https://doi.org/10.3390/geosciences9040147>
- Kou W, Xiangming X, Jinwei D, Shu G, Deli Z, Geli Z, Yuanwei Q, Li L. Mapping deciduous Rubber plantation areas and stand ages with PALSAR and Landsat Images. *Remote Sens.* 2015;7:1048-73. <https://doi.org/10.3390/rs70101048>
- Lupatini M, Semioti Jacques RJ, Antonioli ZI, Suleiman AKA, Fulthorpe RR, Roesch LFW. Land-use change and soil type are drivers of fungal and archaeal communities in the Pampa biome. *World J. Microbiol.* 2013;29:223-33. <https://doi.org/10.1007/s11274-012-1174-3>
- Martins D, Cassol EA, Eltz FLF, Bueno AC. Erosividade e padrões hidrológicos das chuvas de Hulha Negra, Rio Grande do Sul, Brasil, com base no período de 1956 a 1984. *Pesq Agrop Gaúcha.* 2009;15:29-38.
- Minella JPG, Merten GH, Ruhoff AL. Utilização de métodos de representação espacial para cálculo do fator topográfico na equação universal de perda de solo revisada em bacias hidrográficas. *Rev Bras Cienc Solo.* 2010;34:1455-62. <https://doi.org/10.1590/S0100-06832010000400041>
- Moore ID, Burch GJ. Physical basis of the length-slope factor in the universal soil loss equation. *Soil Sci Soc Am J.* 1986;50:1294-8. <https://doi.org/10.2136/sssaj1986.03615995005000050042x>
- Moura-Bueno JM, Dalmolin RSD, Miguel P, Horst TZ. Erosion in hillside areas with fragile soils and their relation to soil cover. *Sci Agrar.* 2018;19:102-12. <https://doi.org/10.5380/rsa.v19i1.53738>
- Nachtigall SD, Nunes MCM, Moura-Bueno JM, Lima CLR, Miguel P, Beskow S, Silva TP. Spatial modeling of soil water erosion associated with agroclimatic seasonality in the southern region of Rio Grande do Sul, Brazil. *Eng Sanit Ambient.* 2020;25:933-46. <https://doi.org/10.1590/s1413-4152202020190136>
- Napoli M, Cecchi S, Orlandini S, Mugnai G, Zanchi CA. Simulation of field measured soil loss in Mediterranean hilly areas (Chianti, Italy) with RUSLE. *Catena.* 2016;145:246-56. <https://doi.org/10.1016/j.catena.2016.06.018>
- Peñalva-Bazzano MG, Eltz FLF, Cassol EA. Erosividade, coeficiente de chuva, padrões e período de retorno das chuvas de Quaraí, RS. *Rev Bras Cienc Solo.* 2007;31:1205-17. <https://doi.org/10.1590/S0100-06832007000500036>
- Ray LK. Limitation of automatic watershed delineation tools in coastal regions. *Ann GIS.* 2018;24:261-74. <https://doi.org/10.1080/19475683.2018.1526212>
- Renard KG, Foster GR, Weisies GA, McCool DK, Yoder DC. Predicting soil erosion by water: A guide to conservation planning with the Revised Universal Soil Loss Equation (RUSLE). Washington, DC: United States Department of Agriculture; 1997.
- Rutebuka J, De Taeye S, Kagabo D, Verdoodt A. Calibration and validation of rainfall erosivity estimators for application in Rwanda. *Catena.* 2020;190:e104538. <https://doi.org/10.1016/j.catena.2020.104538>
- Santos HG, Jacomine PKT, Anjos LHC, Oliveira VA, Lumberras JF, Coelho MR, Almeida JA, Araújo Filho JC, Oliveira JB, Cunha TJF. Sistema brasileiro de classificação de solos. 5. ed. rev. ampl. Brasília, DF: Embrapa; 2018.
- Santos TEM, Montenegro AAA. Erosividade e padrões hidrológicos de precipitação no Agreste Central pernambucano. *Rev Bras Eng Agri Amb.* 2012;16:871-80. <https://doi.org/10.1590/S1415-43662012000800009>

- Sartori A, Lombardi Neto F, Genovez AM. Classificação hidrológica de solos brasileiros para a estimativa da chuva excedente com o método do serviço de conservação do solo dos Estados Unidos Parte 1: Classificação. *Rev Bras Recur Hid.* 2005;10:5-18. <https://doi.org/10.21168/rbrh.v10n4.p5-18>
- Steinmetz AA, Cassalho F, Caldeira TL, Oliveira VA, Beskow S, Timm LC. Assessment of soil loss vulnerability in data-scarce watersheds in southern Brazil. *Cienc Agrotec.* 2018;42:575-87. <https://doi.org/10.1590/1413-70542018426022818>
- Sudhishri S, Kumar A, Singh JK, Dass A, Nain AS. Erosion tolerance index under different land use units for sustainable resource conservation in a Himalayan watershed using remote sensing and geographic information system (GIS). *Afr J Agric Res.* 2014;9:3098-110. <https://doi.org/10.5897/AJAR2013.7933>
- Swarnkar S, Malini A, Tripathi S, Sinha R. Assessment of uncertainties in soil erosion and sediment yield estimates at ungauged basins: an application to the Garra River basin, India. *Hydrol Earth Syst Sci.* 2018;22:2471-85. <https://doi.org/10.5194/hess-22-2471-2018>
- Thomas J, Joseph S, Thirvikramji KP. Estimation of soil erosion in a rain shadow river basin in the southern Western Ghats, India using RUSLE and transport limited sediment delivery functions. *Int Soil Water Conserv. Res.* 2018;6:111-22. <https://doi.org/10.1016/j.iswcr.2017.12.001>
- Zanchin M. Soil loss and sediment delivery estimated by RUSLE and SEDD models in a subtropical climate' watershed [dissertation]. Pelotas: Universidade Federal de Pelotas; 2020.
- Zanin PR, Bonumá NB, Minella JPG. Determination the topographic factor in watershed. *Rev Bras Geomorfol.* 2017;18:19-36. <https://doi.org/10.20502/rbg.v18i1.1023>
- Zhu X, Zhang R, Sun X. Spatiotemporal dynamics of soil erosion in the ecotone between the Loess Plateau and Western Qinling Mountains based on RUSLE modeling, GIS, and remote sensing. *Arab J Geosci.* 2021;14:33. <https://doi.org/10.1007/s12517-020-06329-z>
- Wischmeier WH, Smith DD. Predicting rainfall erosion losses: A guide to conservation planning. Washington, DC: Agriculture Handbook; 1978.
- Wollmann CA. The floods in Rio Grande do Sul during 21th century. *Mercator.* 2014;13:79-91. <https://doi.org/10.4215/RM2014.1301.0006>